AD-A169 603 NEW RESULTS ON LOW TEMPERATURE THERMAL OXIDATION OF SILICON(U) NORTH CAROLINA UNIV AT CHAPEL HILL DEPT OF CHEMISTRY E A IRENE 20 JUN 86 TR-5 N00014-83-K-0571 1/1

UNCLASSIFIED F/G 7/4 NL

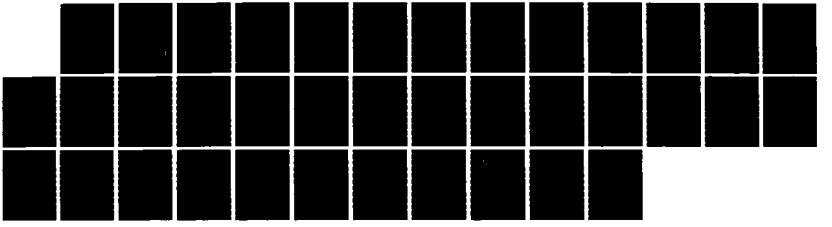

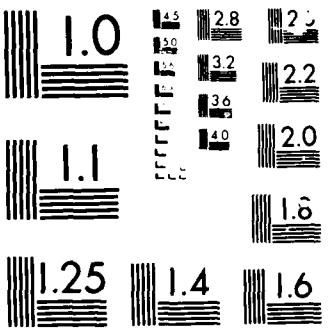
1.0
1.1
1.25
1.4
1.6
2.8
3.2
3.6
4.0
2.2
2.0
1.8

OFFICE OF NAVAL RESEARCH

Contract No. N00014-83-K-0571

Task No. NR 625-843

TECHNICAL REPORT NO. 5

# New Results on Low Temperature Thermal Oxidation of Silicon

by

E.A. Irene
Dept. of Chemistry
The University of North Carolina
Chapel Hill, NC 27514

in

Philosophical Magazine (U.K.)

ADA 169603

SECURITY CLASSIFICATION OF THIS PAGE

## REPORT DOCUMENTATION PAGE

| | |
|---|---|
| 1a REPORT SECURITY CLASSIFICATION: Unclassified | 1b. RESTRICTIVE MARKINGS |
| 2a SECURITY CLASSIFICATION AUTHORITY | 3. DISTRIBUTION/AVAILABILITY OF REPORT: Approved for public release; distribution unlimited. |
| 2b DECLASSIFICATION/DOWNGRADING SCHEDULE | |
| 4 PERFORMING ORGANIZATION REPORT NUMBER(S): Technical Report #5 | 5. MONITORING ORGANIZATION REPORT NUMBER(S) |
| 6a NAME OF PERFORMING ORGANIZATION: UNC Chemistry Dept. / 6b. OFFICE SYMBOL (If applicable) | 7a. NAME OF MONITORING ORGANIZATION: Office of Naval Research (Code 413) |
| 6c. ADDRESS (City, State and ZIP Code): 11-3 Venable Hall 045A, Chapel Hill, NC 27514 | 7b. ADDRESS (City, State and ZIP Code): Chemistry Program, 800 N. Quincy Street, Arlington, Virginia 22217 |
| 8a NAME OF FUNDING/SPONSORING ORGANIZATION: Office of Naval Research / 8b. OFFICE SYMBOL (If applicable) | 9. PROCUREMENT INSTRUMENT IDENTIFICATION NUMBER: Contract N00014-83-K-0571 |
| 8c. ADDRESS (City, State and ZIP Code): Chemistry Program, 800 N. Quincy, Arlington, VA 22217 | 10 SOURCE OF FUNDING NOS: PROGRAM ELEMENT NO / PROJECT NO / TASK NO: NR625-843 / WORK UNIT NO |
| 11 TITLE (Include Security Classification): NEW RESULTS ON LOW TEMPERATURE THERMAL OXIDATION OF SILICON | |
| 12 PERSONAL AUTHOR(S): F.A. Irene | |
| 13a TYPE OF REPORT: Interim Technical / 13b TIME COVERED: FROM _____ TO _____ | 14 DATE OF REPORT (Yr, Mo, Day): 6/20/86 / 15 PAGE COUNT: 34 |
| 16 SUPPLEMENTARY NOTATION: Prepared for publication in Philosophical Magazine (U.K.) | |
| 17 COSATI CODES: FIELD / GROUP / SUB GR | 18 SUBJECT TERMS (Continue on reverse if necessary and identify by block number): Silicon Oxidation; Silicon Dioxide Properties; Thin Film Growth Models |

19 ABSTRACT (Continue on reverse if necessary and identify by block number)

The commonly accepted linear-parabolic oxidation model for the thermal oxidation of Si includes two rate processes in a steady state: reaction between Si and oxidant at the $Si-SiO_2$ interface; and transport of oxidant through the $SiO_2$ film. Based on available data, it is argued that the former process seems dominant for thin film growth in dry $O_2$. A number of measured $SiO_2$ film and $Si-SiO_2$ interface measured properties are reported, as well as the variation of the these properties with oxidation temperature and Si substrate orientation. These properties include; refractive index, density, intrinsic stress, interface fixed oxide charge and interface trapped charge. It is also observed that all of these properties display similar oxidation temperature and inert anneal behavior plus a complex orientation dependence. Through the use of a modified form for the interface reaction, a better understanding is obtained of both the origin of these measured properties, and new oxidation data taken on five Si orientations and at lower oxidation temperatures than previously reported.

| | |
|---|---|
| 20 DISTRIBUTION/AVAILABILITY OF ABSTRACT: UNCLASSIFIED/UNLIMITED ☒ SAME AS RPT ☒ DTIC USERS ☐ | 21 ABSTRACT SECURITY CLASSIFICATION: Unclassified |
| 22a NAME OF RESPONSIBLE INDIVIDUAL: Dr. David L. Nelson | 22b TELEPHONE NUMBER (Include Area Code): (202) 696-4410 / 22c OFFICE SYMBOL |

DD FORM 1473, 83 APR EDITION OF 1 JAN 73 IS OBSOLETE

SECURITY CLASSIFICATION OF THIS PAGE

# New Results On Low Temperature Thermal Oxidation Of Silicon



by

E. A. Irene

Department of Chemistry

University of North Carolina

Chapel Hill, North Carolina 27514

U.S.A.



The commonly accepted linear-parabolic oxidation model for the thermal oxidation of Si includes two rate processes in a steady state: reaction between Si and oxidant at the Si-$SiO_2$ interface; and transport of oxidant through the $SiO_2$ film. Based on available data, it is argued that the former process seems dominant for thin film growth in dry $O_2$. A number of measured $SiO_2$ film and Si-$SiO_2$ interface measured properties are reported, as well as the variation of the these properties with oxidation temperature and Si substrate orientation. These properties include: refractive index, density, intrinsic stress, interface fixed oxide charge and interface trapped charge. It is also observed that all of these properties display similar oxidation temperature and inert anneal behavior plus a complex orientation dependence. Through the use of a modified form for the interface reaction, a better understanding is obtained of both the origin of these measured properties, and new oxidation data taken on five Si orientations and at lower oxidation temperatures than previously reported.

The study of the thermal oxidation of single crystal silicon remains an important area of research within the field of electronic materials. This is so because of both the technological relevance of the Si-$SiO_2$ interface (1,2) with the associated important scientific questions pertaining to oxide film growth kinetics (3,4), and the general questions pertaining to the origin and control of electronics properties of semiconductor surfaces.

The present paper first compares the relative role of the interface reaction between Si and oxidant at the Si-$SiO_2$ interface with the transport of oxidant by steady state Fickian diffusion to the interface. Using available diffusivity values, D, parabolic rate constants, $k_p$, and oxidation rate data, $\dot{L}$, (5-7), it is found that the interface reaction for Si oxidation is dominant up to at least several tens of nm of $SiO_2$ film growth with oxidation temperatures from 600°C up to 1000°C in 1 atm dry $O_2$. Secondly, we report the measurement of a number of physical properties for $SiO_2$ films on Si substrates: $SiO_2$ film density, refractive index, intrinsic film stress and fixed oxide and interface trapped charge. Some of these measurements are recently reported, others have been in the literature. The oxidation temperature dependence for all of these properties is qualitatively the same, and strongly suggests a common origin. Thirdly, we consider the interface reaction between Si and oxidant and deduce a model for this reaction to explain initial oxidation kinetics. New oxidation data (6,7) is presented that shows some agreement with the model which explicitly considers both the areal density of Si atoms on various Si surfaces and the intrinsic stress. The stress is compressive in $SiO_2$, thereby reducing the diffusivity of oxidant through the $SiO_2$ film; and the stres is tensile in Si, thereby enhancing the reactivity of the Si surface, if there is any effect of stress at all. Experimental detail is treated in separate publications; only a brief summary of

relevant experimental results are presented herein.

## I. The Initial Regime

There are numerous publications (8-10) which attempt to consider the transport of oxidant to be always rate limiting for the oxidation of Si. We find, however, that this assumption is not justified and we base our conclusion on a comparison of the calculated diffusion flux with the actual oxidation rate. Using available data for D, $k_p$ and $\dot{L}$ and the assumption of steady state Fickian diffusion, the diffusion flux of $O_2$, F(D), is given by:

$$F(D) = D_{O_2}(C_1-C_2)/L$$

where $C_1$ is the solubility of $O_2$ in $SiO_2$ and $C_2$ is the $O_2$ concentration at the Si-$SiO_2$ interface. We assume that the solubility of $O_2$ in $SiO_2$ is constant with temperature and has the value $C_1 = 5 \times 10^{16} cm^{-3}$ (11). We need to realize that the D values of Norton (5) were obtained at high temperatures and using bulk $SiO_2$ glass, and thus cannot be readily extrapolated to thin films of pure $SiO_2$ prepared at temperatures below 900°C where the intrinsic compressive stress (12,13) may seriously decrease D (8-10). For these lower temperatures, we calculate D from the available $k_p$ data (6) and with the use of the Deal and Grove(11) expression for D as:

$$D = Nk_p/2C_1$$

where N is the number density of $O_2$'s in $SiO_2$. This method of calculating D values for lower temperature oxidation is in accord with the experimentally obtained curvature of the

ln $k_p$ vs. 1/T plot(14) which shows a negative deviation to the linearity extrapolated from high temperatures to the lower temperatures (below 900°C). This results in a smaller value for D than the values extrapolated from Nortons data. We assume $C_2$ is very small relative to $C_1$ and can therefore be ignored.

We compare this diffusive flux, F(D), with the flux of $O_2$ calculated using the experimental $SiO_2$ growth rates, F(exp). A ratio, R, is formed:

$$R = F(D)/F(exp)$$

This ratio has the following characteristics:

$R = 1$ Diffusion control

$R > 1$ Interface control

$R < 1$ *Impossible*

and can therefore be used to indicate the dominant kinetic process. When the diffusion flux fully accounts for the actual film growth rate then diffusion is the rate limiting process and R = 1. When the calculated diffusion flux is larger than is necessary to account for the measured oxidation rate, $\dot{L}$, then the oxidation mechanism is under interface reaction control and R > 1. The diffusive supply function can never yield less $O_2$ than is required by $\dot{L}$ hence R < 1 is not possible for our situation as defined. The results of this calculation are displayed in Table 1. It is seen that R is always greater than unity for oxidation temperatures of from 600°C to 1000°C and up to at least several tens of nm which comprises the initial fast oxidation regime. Therefore, based on the available data and simple ideas of transport and reaction, we conclude that the reaction

at the Si - $SiO_2$ interface is likely to be rate limiting. There exists other supporting evidence for this position. For example, the oxide intrinsic stress is compressive in $SiO_2$ and tensile in Si. Thus if there is any effect of stress for thin films, the stress should decrease the diffusivity by decreasing the free volume in the $SiO_2$(8-10), and increase the surface reactivity by stretching the Si bonds. We actually observe an enhanced initial oxidation rate relative to the kinetics for thick films which seems to support the interface reaction effects. Also, if the diffusivity is rate limiting and affected by stress, then in the early stage of oxidation the diffusivity must be smaller than for thick films where some oxide has viscoelastically relaxed, yet a larger initial rate is observed for dry $O_2$ oxidation.

## II. Physical Properties Measurements

We have measured several physical properties of $SiO_2$ films on Si and there exists a number of similar measurements in the literature. We select for display in this paper only those properties whose values we have confirmed, and more importantly, we show the variation of these properties with oxidation temperature.

Figure 1 shows the measurement of the real part of the refractive index for $SiO_2$ as a function of oxidation temperature. This was assumed by Taft to be a result of an increased oxide density (15). Later measurement of the index and density (16) revealed almost exactly the same values for the refractive index, n, as Taft. While the density measurement was not nearly as accurate, a definite increase was found in the measured density for the lower oxidation temperatures. Figure 2 shows the results of converting the n values to densities, $\rho$, through the Lorentz - Lorentz equation:

$$\rho = K(n^2-1)/(n^2+2)$$

and in order to calculate K, literature values for n at measured $\rho$ were used (17) from which a value of K = 8.0461 was obtained.

Further evidence for densification was recently obtained using infrared spectroscopy techniques (18). Figure 3 shows a typical set of spectra from which the dominant change is a shift in the $1077cm^{-1}$ band to lower frequencies with decreasing oxidation temperatures. This band is attributed to the in plane stretching of Si-O-Si and the shift has been attributed to a decrease in the Si-O-Si bond angle which is anticipated for densification (19).

Figure 4 shows the results of intrinsic film stress measurements on $SiO_2$ films on Si (20,21). The details of the actual stress measurement technique and thermal stress corrections were published separately along with the experimental results (20,21). These results agree essentially with previous independent measurements (12,13). We observe an increase in the compressive $SiO_2$ intrinsic stress with decreasing oxidation temperatures for all orientations. For reasons to be discussed later, the (111) yields the smallest stress, although this orientation is anticipated to yield the largest stress on a planar Si surface. The film stress, $\sigma$, in the elastic limit is given as:

$$\sigma = E\epsilon$$

where E is Young's modulus and $\epsilon$ is the strain which is the change in volume divided by the volume, $\delta V/V$. The orientation dependence of $\sigma$ is obtained from only the orientation dependence of E (or better $E/(1-\nu)$ where $\nu$ is Poisson's ratio), since the volume change, $\delta V$, due to oxidation is the same for all orientations. Table 2 shows the calculation of $E/(1-\nu)$ values for various Si orientations (7). From this table and the above

relationship, we deduce that the order for the stress on the various Si orientations should be:

$$\sigma_{111} > \sigma_{110} > \sigma_{100}.$$

However, we measure the order for the stresses to be:

$$\sigma_{110} \geq \sigma_{100} > \sigma_{111}.$$

Later we discuss both the possible reasons for this order change, and more importantly for our present purpose are the implications of this experimentally determined orientation dependence of the intrinsic stress on Si oxidation kinetics.

The remaining physical properties reported here include the fixed oxide charge, $Q_f$, and interface trapped charge, $Q_{it}$. The former charge, $Q_f$, is associated with excess Si at the $Si-SiO_2$ interface while $Q_{it}$ is the charge trapped in surface electronic states. These surface states are thought to be a result of unsatisfied or dangling bonds at the Si surface. Fig. 5 is a pictorial representation of the trend observed for $Q_f$ and $Q_{it}$ with oxidation temperature (22,23). Both of these kinds of charges have been found to anneal to lower values, but quite complex chemical effects are sometimes observed for $Q_{it}$.

It is important to realize that all the properties thus far discussed decrease in value with inert gas annealing (16,21-23). Also, all the property values are lower for oxides grown in an $H_2O$ containing ambient. The rate of decrease of the property seems to depend on the temperature of the anneal. It therefore appears that there is a relaxation upon annealing which is strongly suggestive of viscoelastic behavior(12,13,15).

Fig. 6 summarizes all the herein reported physical property results. With this similar behavior of the properties with oxidation behavior, we believe that a common origin is strongly suggested. We consider that the stress is the most fundamentally related property to the oxidation reaction through the change in the molar volume, $\delta V$. This change in volume causes the $SiO_2$ to increase in density through two mechanisms. One is a simple compression due to the existence of a residual stress as measured. This effect is quantified from the stress optical coefficient for $SiO_2$ (24).

$$dn/d\sigma = 9 \times 10^{-13} \text{ cm}^2/\text{dyne}$$

From this coefficient, we can only account for less than half of the observed change in n. The remaining densification may be due to structural changes, perhaps an alteration of the ring statistics (25). This latter effect may account for the lack of complete annealing of some of the properties(21). The rationale used here is that the stress induced components that require the continual existence of the stress are annealed as the stress is annealed, but the structural changes that required stress initially and for relaxation require bond breaking, are less likely to anneal quickly or completely.

With Part I indicating the importance of the interface reaction and Part II demonstrating that a number of properties related to the film stress change with decreasing oxidation temperature, we now use the effect of stress on the interface reaction between oxidant and Si to attempt to correlate previously published and newly obtained oxidation data.

## III. Oxidation Kinetics

In this part, we firstly present oxidation data of Massoud et al. (6) which shows a crossover effect with various Si orientations. Fig. 7a and b shows that initially the (110) orientation has the greatest rate of oxidation, but at thickness greater than 20 nm the (111) is dominant. Previously, we attempted to explain this phenomenon (25) based on a recent revision (26) to the linear - parabolic model (11). Only the essential features of the revised model as it pertains to the initial regime will be reproduced here. Fig. 8 shows that as the oxide grows, the molar volume change $\delta V$ and the adhesion to the Si surface cause the development of a compressive oxide stress (tensile in the Si surface) and a viscous flow in the normal direction which is parallel to the $SiO_2$ growth direction. Using this picture, and starting from the Deal-Grove (11) interface reaction flux:

$$F = k_1 C_2$$

where $k_1$ is first order rection rate constant and $C_2$ is the concentration of oxidant at the $Si-SiO_2$ interface, we modify this flux by explicitly expressing the available number of Si atoms on the Si surface, $C_{Si}^*$, as:

$$F = k' C_2 C_{Si}^*$$

and $C_{Si}^*$ is obtained directly from the geometric areal density of Si atoms on a given surface, $C_{Si}$, by multiplying $C_{Si}$ by a fraction. Considering $SiO_2$ as a Maxwell solid, we assume that this fraction is the strain rate, $\dot{\epsilon}$ as:

$$\dot{\epsilon} = \sigma / 1\eta$$

where $\sigma$ is the stress and $\eta$ the oxide viscosity. This means that the rate at which the $SiO_2$ relaxes into the growth direction influences the rate at which the oxidation reaction will proceed. Then the following form for $k_1$ from the Deal-Grove expression is obtained:

$$k_1 = k' C_{Si} \sigma / \eta$$

It should be realized that this modified expression for $k_1$ is obtained by simply assuming that stress affects the interface reaction and that the number of Si atoms on the surface is also infuencing the oxidation rate in the early regime. Even if our assumptions are entirely correct, it is quite likely that the form for the rate expression will require modification as more data is revealed. However, this simple formulation will enable a scaling with the oxidation data and in particular the crossover effect shown above.

In order to explain the Massoud et al. (6) data using the relationship above, we assume that in the earliest stage of oxidation, the primary factor is the areal density of Si atoms. As seen in Table 3, the oxidation order from this is:

$$(110) > (111) > (100)$$

and this scales with the data. As the oxide film grows, the third dimension of the $SiO_2$ network develops, and with this we should anticipate the film to exert itself mechanically. Using the revised form for $k_1$, we would then expect the stress to dominate. At the time we submitted this work for publication(26), we did not haveaccess to the measured stress values in Figure 4, and thus we relied on the calculated stress, thereby anticipating that the order of the oxidation kinetics based on stress should be:

(111) > (110) > (100)

which is as observed for the oxide grown thicker than the crossover. Of course, now with the stress measurements as a function of Si orientation (Figure 4), we find that this order is not correct. Also, we have now added two new orientations, the (311) and (511), which according to Table 3 and the atom counting procedure of Ligenza (28) should have a greater areal density of Si and hence a greater initial oxidation rate. This new oxidation rate data which includes these additional Si orientations is shown in Figure 9. We observe that the (511) and (311) rates are respectively further above the (100) rate, but both are below the (111) rate. Ligenza presumably considered the (511) and (311) to be simple atomic planes and counted the atoms on or near the plane. In fact, however, the (511) and (311) planes are vicinal planes to the (100) and (111) (29). As such, both of these planes are composed of a combination of (100) terraces and (111) ledges in ratios so as to yield the proper inclination to the (100) plane. The proportion of (111) steps increases from (511) to (311) to eventually produce the (111) and the oxidation rate scales similarly. Thus we continue to believe that the initial oxidation rate scales with the areal density of atoms, and that apparently an error exists in the literature for the areal density for the (311) plane.

According to the revised interface reaction expression, the stress at the Si surface should also be important. Indeed, the product $C_{Si}\sigma$ ought to be determined through the linear rate constant. However, Table 4 shows that this product is anomolously low for the (111) surface. Since the very initial rate scales with $C_{Si}$, we continue to support the previous assumption that the stress in the very initial stage is not important. We previously argued (26) that this was so because the film was too thin to mechanically exert itself until the third dimension grows adequately thick and hence to develop

mechanical properties. Other possible explanations are that the stress for very thin films is different than for the films of greater than 100 nm as in Figure 4. We have commenced experiments directed at films less than 20 nm. Also, as stated above, the form for the revised rate constant may not be correct. Another possibility is that the low stress for the (111) surface may be responsible for an enhanced rate due to an enhanced diffusivity rather than an effect on the surface reaction kinetics. Evidence for this is given in Table 5 which contains a set of parabolic rate constants from Massoud et al. (6). These constants show that for lower temperatures, the $k_p$ values for the (111) actually increase above those for the (110) and (100) orientations thus indicating the importance of transport but somehow orientation dependent transport. Of course, since these $k_p$ values originate with the Deal-Grove model, they are model dependent parameters and are therefore only as reliable as the model.

Lastly, we return to the stress measurements and the possible reasons why the (111) exhibits a lower stress than anticipated from E/1-v values as shown in Table 3. The anticipated stress values assumed a planar Si surface. Mott (30) has suggested that if oxidation proceeds at surface steps, the resulting stress would be considerably reduced because a part of the $\delta V$ is relieved by the receeding Si step as shown in Figure 10. Hahn and Henzler (31) report that among a rather wide list of process parameters that alter the surface step density on Si surfaces, they measure a significantly greater density of steps as the (111) compared to the (100) surface. This finding lends considerable support to the application of the model proposed by Mott. Contained within the papers at this workshop is one of particular application to the present research presented by Leroy (32) which quantitatively explains the experimentally found orientation dependence of the stress. While we do not reproduce the Leroy arguments here as the paper is published simultaneously with the present paper, a brief summary is in order. The Leroy model

considers that the first oxidation event creates a step on the Si surface, since Si on the surface is replaced with $SiO_2$. Once a step is produced, the forces resulting from the oxidation induced $\delta V$ will be manifest in the residual measured intrinsic stress according to the resolved component of the biaxial stress in the Si surface. This stress requires resolution in the direction of the slip plane in relation to its angle with the Si surface. This angle is orientation dependent. The resulting stress, $\sigma_c$ is compared to the critical shear stress, $\tau_c$. When $\sigma_c$ exceeds $\tau_c$, defects are produced and stress is relieved. Leroy calculates, quantitatively, the relative order for the (100), (110), (111) and (311) stresses using these ratios for the different Si orientations of this study. He considers that any defects produced are rapidly removed by oxidation. There are further profound implications of the Leroy model and the reader is referred to the paper (32).

Summary and Conclusions

Using available data for D, $k_p$ and $\dot{L}$ and simple calculations, we conclude that the interface reaction between Si and oxidant is important for the early thermal oxidation regime. Other evidence such as possible stress effects and the apparent non-physical results obtained by using the interface reaction further strengthen this approach. A variety of $SiO_2$ and Si-$SiO_2$ physical properties have very similar oxidation temperature behavior and the property values relax to lower values upon inert anneal. This suggests that the properties have a common origin and we believe that the development of the stress is the common cause for the temperarture dependence of the properties. The anneal behavior suggests the viscoelastic nature of the $SiO_2$ films. A revised linear rate constant is employed along with new oxidation data that includes five Si orientations to understand the low temperature oxidation phenomena. The importance of the areal density of Si atoms

appears to be a strong correlation for the very initial regime and is contained explicitly in the revised interface model. The observed crossover seems to be due to stress transport effects if the data is explained within the proposed revised model. While the revised interfacial reaction model has some physical appeal, more research is needed to prove or disprove this model and to arrive at a better description of the early stage of thermal oxidation of Si.

Acknowledgements

This research was supported in part by the Office of Naval Research, ONR. The author gratefully acknowledges enlightening discussions, access to original research results and collaboration with E.A. Lewis, E. Kobeda, J.K. Srivastava, G. Lucovsky, and F.M. d'Heurle.

## References


1. E.H. Nicollian and J.R. Brews, "MOS (Metal Oxide Semiconductor) Physics and Technology," John Wiley and Sons, 1982.

2. E.A. Irene, Semiconductor International, April 1983, p. 99 and June 1985, p. 92.

3. J.M. Aitken and E.A. Irene, "Silicon Dioxide Films in Semiconductor Devices," in "Treatise on Materials Science and Technology," Vol. 26, Eds. M. Tomozawa and R.H. Doremus, p. 1, Academic Press, 1985.

4. E.A. Irene, "Silicon Oxidation: A Process Step for the Manufacture of Integrated Circuits," in "Integrated Circuits," Ed. P. Stroeve, p. 31, American Chemical Society, 1985.

5. F.J. Norton, Nature, 191, 701 (1961).

6. H.Z. Massoud, J.D. Plummer and E.A. Irene, J. Electrochem. Soc., 132, 1745, 2685, 2693 (1985).

7. E.A. Lewis, E. Kobeda and E.A. Irene, Proc. of Fifth Int'l Symp. on Silicon Matl's. Science and Technol., Eds. H.R. Huff, T. Abe and B. Kolbesen, Electrochem. Soc., 1986, p. 416.

8. A. Fargeix and G. Ghibaudo, J. Appl. Phys., 56, 589 (1984).

9. G. Camera Roda, F. Santarelli, and G.C. Sarti, J. Electrochem. Soc., 132, 1909 (1985).

10. R.H. Doremus, Thin Solid Films, 122, 191 (1984).

11. B.E. Deal and A.S. Grove, J. Appl. Phys., 36, 3770 (1965).

12. E.P. EerNisse, Appl. Phys. Lett., 35, 8 (1979).

13. E.A. Irene, E. Tierney and J. Angillelo, J. Electrochem. Soc., 129, 2594 (1982).

14. E.A. Irene and D.W. Dong, J. Electrochem. Soc., 125, 1146 (1978).

15. E.A. Taft, J. Electrochem. Soc., 125, 968 (1978).

16. E.A. Irene, D. Dong and R.J. Zeto, J. Electrochem. Soc., 127, 396 (1980).

17. W.A. Pliskin, J. Vac. Sci. Technol., 14, 1064 (1977); W.A. Pliskin and H.S. Lehman, J. Electrochem. Soc., 112, 1013 (1965).

18. G. Lucovsky, M. Martini, J.K. Srivastava and E.A. Irene, to be submitted for publication 1986.

19. A.E. Geissberger and F.L. Galeener, Phys. Rev. B, 28, 3266 (1986).

20. E. Kobeda and E.A. Irene, J. Vac. Sci. Technol. B, 4, 720 (1986).

21. E. Kobeda and E.A. Irene, J. Vac. Sci. Technol., submitted for publication 1986.

22. B.E. Deal, M. Sklar, A.S. Grove and E.H. Snow, J. Electrochem. Soc., 114, 266 (1967).

23. R.R. Razouk and B.E. Deal, J. Electrochem. Soc., 126, 1573 (1979).

24. W. Primak and D. Post, J. Appl. Phys., 30, 779 (1959).

25. F.J. Grunthaner and J. Maserjian, "The Physics of $SiO_2$ and It's Interfaces," S.T. Pantelides Ed., Pergamon Press, New York, N.Y., p. 389, 1978.

26. E.A. Irene, H.Z. Massoud and E. Tierney, J. Electrochem. Soc., 133, 1253 (1986).

27. E.A. Irene, J. Appl. Phys., 54, 5416 (1983).

28. J.R. Ligenza, J. Phys. Chem., 65, 2011 (1961).

29. K. Ueda and M. Inoue, Surf. Sci., 161, L578 (1985).

30. N.F. Mott, Proc. Royal Soc. London, A376, 207 (1981).

31. P.O. Hahn and M. Henzler, J. Vac. Sci. and Technol. A, 2, 574 (1984).

32. B. Leroy, "Stresses and Silicon Interstitials During the Oxidation of a Silicon Substrate," presented at workshop on Oxidation Mechanisms at University of Paris 7, May 20 - 22, 1986, Paris, France and to be published in Phil. Mag. 1986/87.

33. E.A. Lewis and E.A. Irene submitted for publication 1986.

## List of Tables

Table 1: Values of R = F(D)/F(exp) at Differing $SiO_2$ Film Thicknesses

| Oxidation Temperature (°C) | R Values at $SiO_2$ Thicknesses (Å) 10 | 50 | 100 | 500 |
|---|---|---|---|---|
| 1000 | 38 | 9 | 5 | 2 |
| 800 | 17 | 10 | 7 | 3 @400Å |
| 700 | 38 | 13 | 8 | |
| 650 | 15 | 9 | 8 | |
| 600 | 10 | | | |

Table 2: Values of E/(1-v) for Si

| Si Orientation | E/(1-v) ($10^{12}$ dyne/cm$^2$)* |
|---|---|
| (100) | 1.805 |
| (110) | 2.187 |
| (111) | 2.290 |
| (311) | 2.007 |

*Reference (7)

Table 3: Areal Density of Si Atoms on Various Orientations

| Si Orientation | Areal Density, $C_{Si}$ ($10^{14}/cm^2$)* |
|---|---|
| (100) | 6.78 |
| (111) | 7.83 |
| (110) | 9.59 |
| (311) | 10.80 |
| (511) | 11.46 |

*counting done after Ligenza in Reference (28)

Table 4: Product of $C_{Si}\sigma$ for Three Si Orientations

| Si Orientation | Product $C_{Si}\sigma$ Relative to (100) |
|---|---|
| (100) | 1 |
| (110) | 1.7 |
| (111) | 0.8 |

Table 5: Parabolic Rate Constants*

| Oxidation Temperature (°C) | $k_p$ ($Å^2$/min.) | | |
|---|---|---|---|
| | (100) | (110) | (111) |
| 1000 | 28,600 | 14,300 | 26,600 |
| 950 | 12,100 | 6,590 | 10,800 |
| 900 | 5,590 | 4,000 | 6,500 |
| 850 | 1,890 | 1,840 | 2,980 |
| 800 | 660 | 855 | 1,350 |
| 750 | 173 | 148 | 4[illegible] |
| 700 | 29 | 29 | 58 |

* from Massoud et al., Reference (6)

## List of Figures

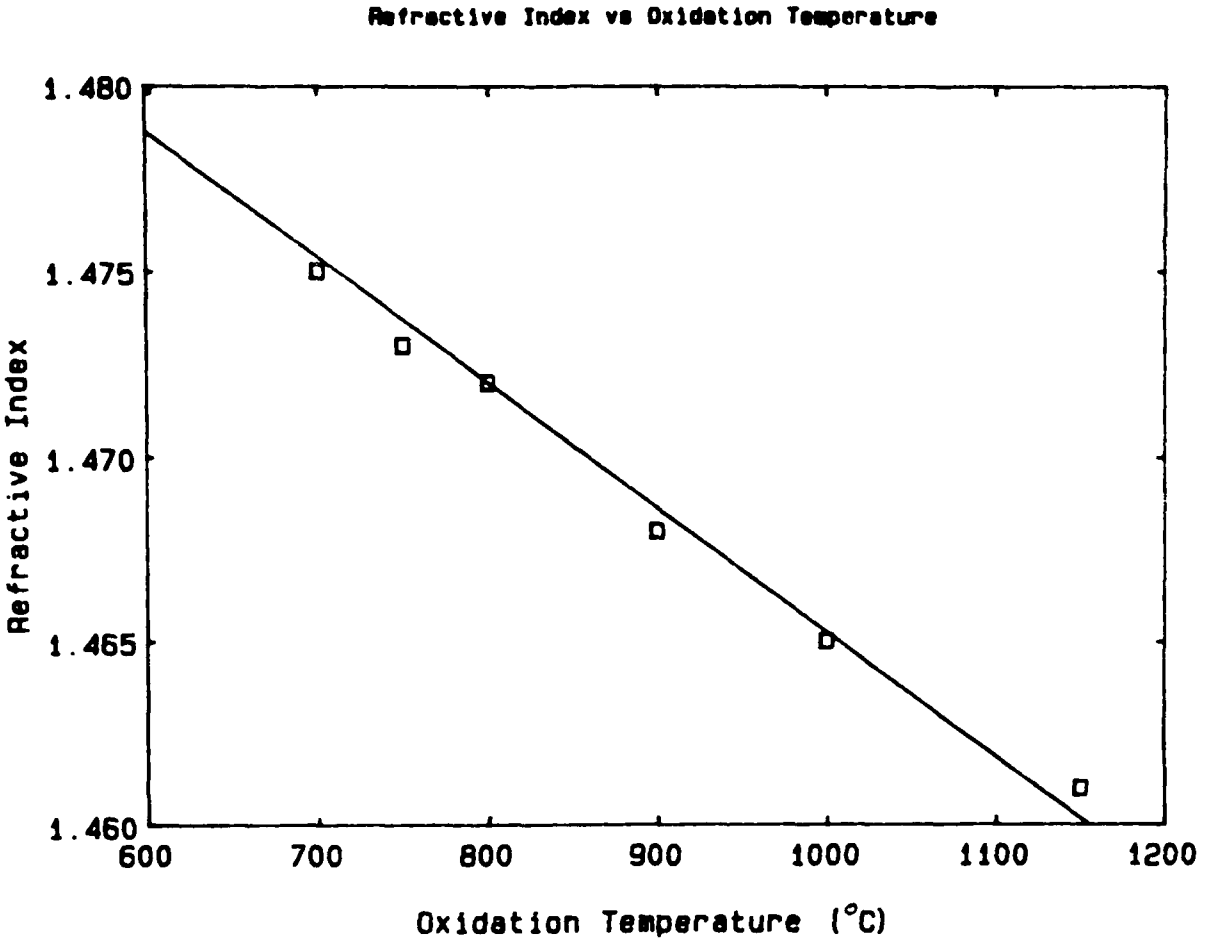
Refractive Index vs Oxidation Temperature
1.480
1.475
1.470
1.465
1.460
Refractive Index
600
700
800
900
1000
1100
1200
Oxidation Temperature (°C)

Fig 1.

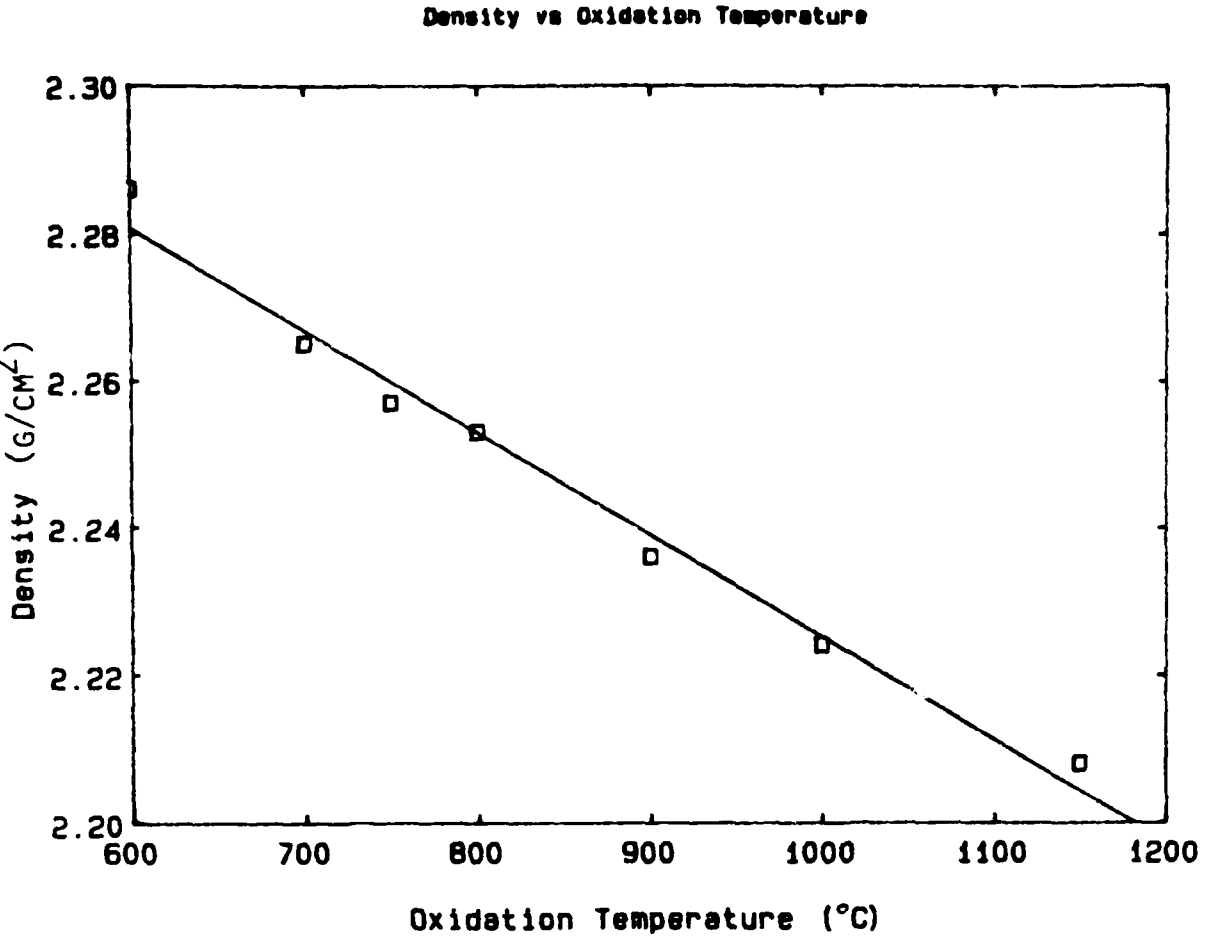
Density vs Oxidation Temperature
2.30
2.28
2.26
2.24
2.22
2.20
Density (G/CM2)
600
700
800
900
1000
1100
1200
Oxidation Temperature (°C)

Fig. 2

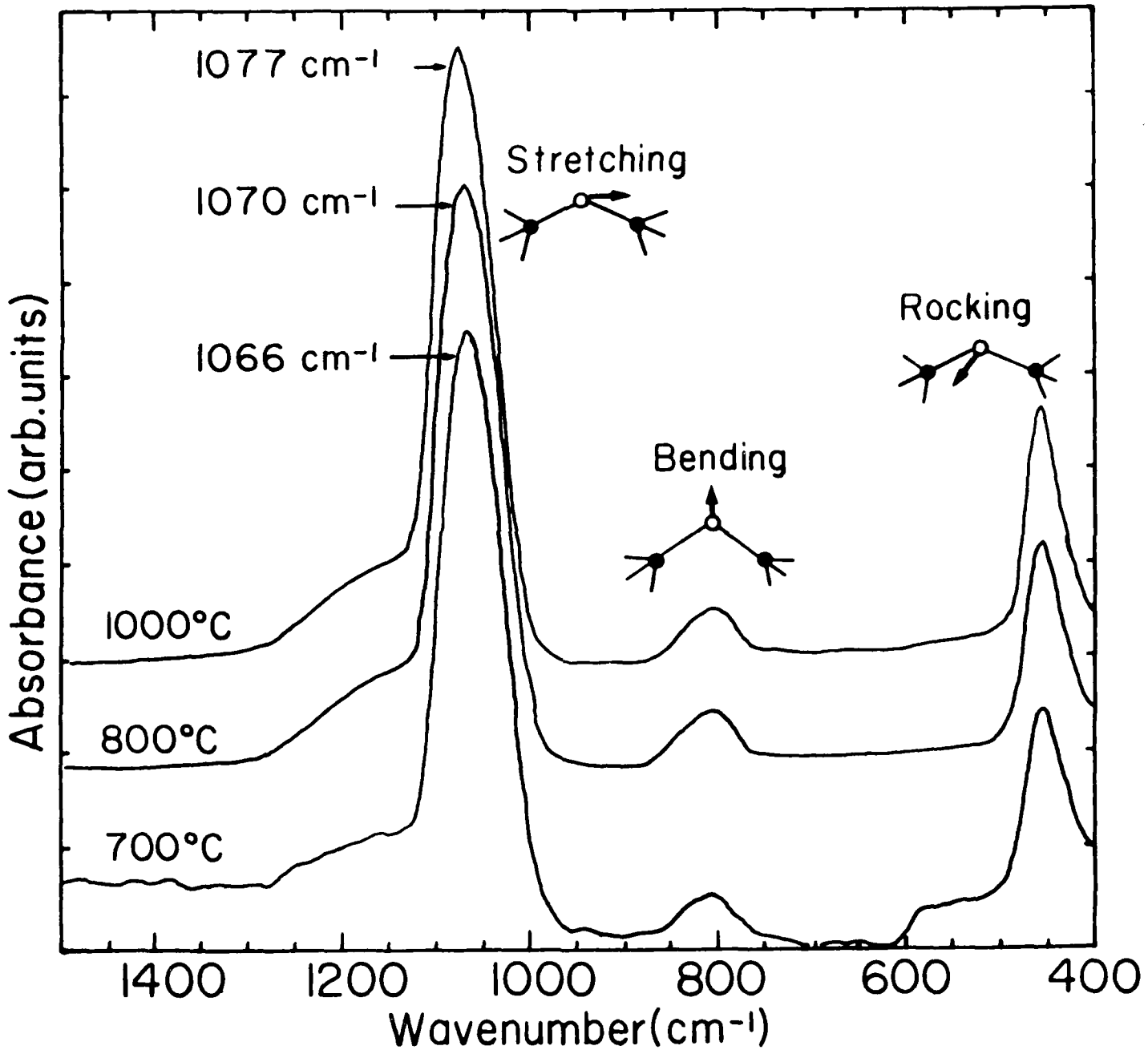
1077 cm⁻¹
1070 cm⁻¹
1066 cm⁻¹
Stretching
Rocking
Bending
1000°C
800°C
700°C
Absorbance (arb.units)
1400
1200
1000
800
600
400
Wavenumber (cm⁻¹)

Fig 3

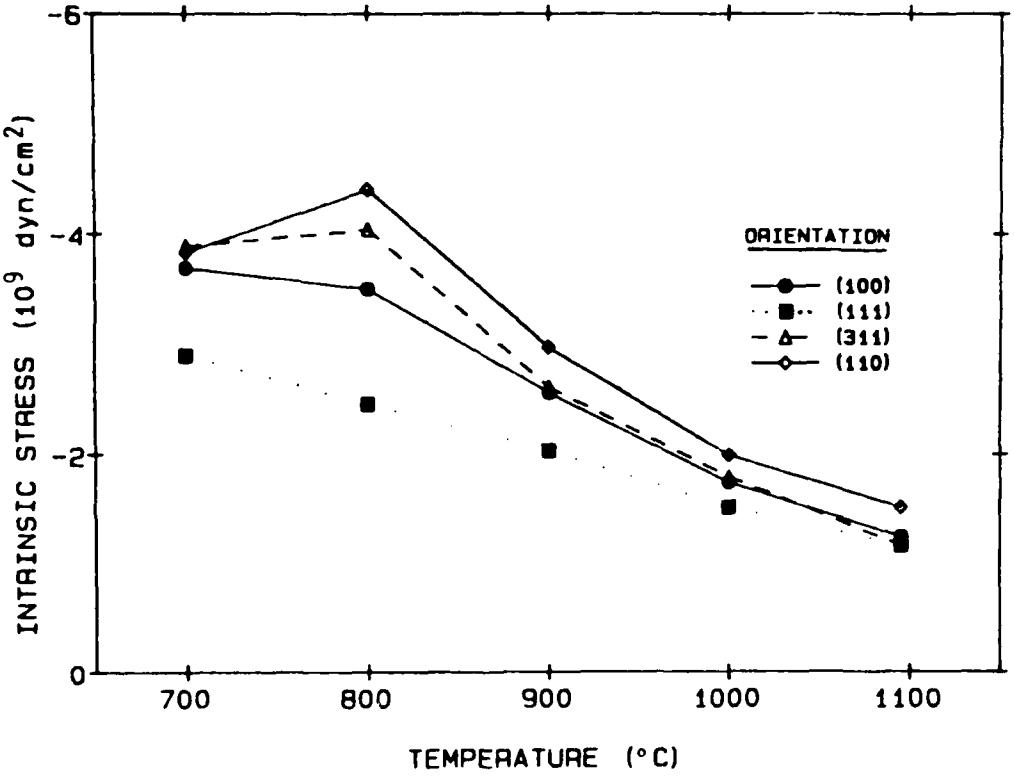
-6
-4
-2
0
INTRINSIC STRESS ($10^9$ dyn/cm$^2$)
700
800
900
1000
1100
TEMPERATURE (°C)
ORIENTATION
(100)
(111)
(311)
(110)

Fig 4

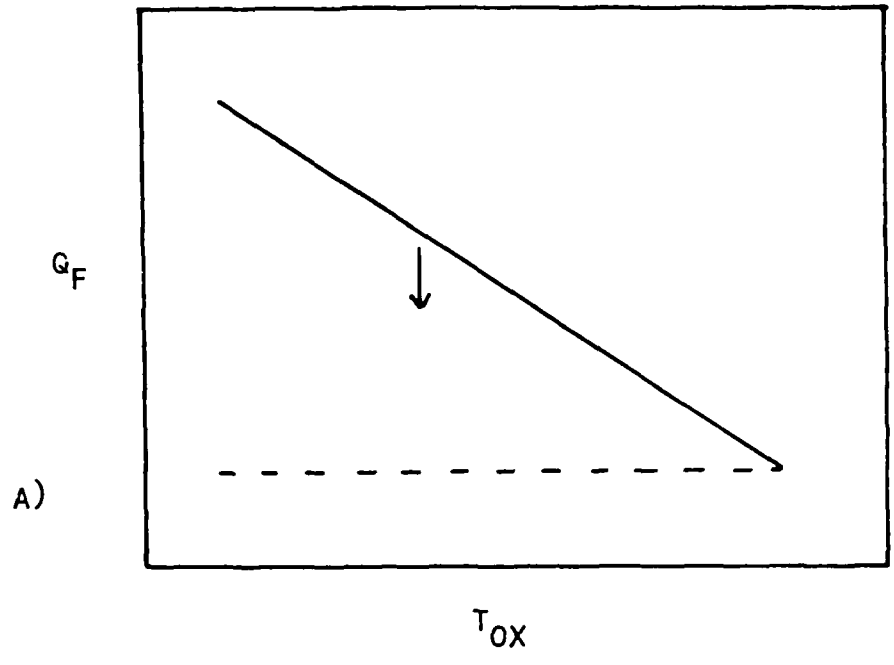


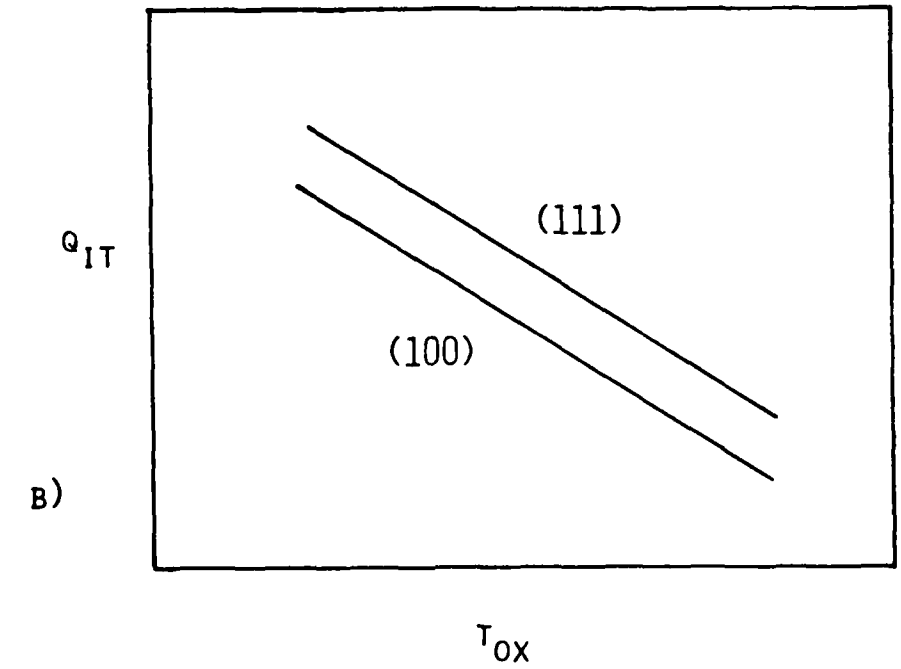


Fig 5

# $SiO_2$ FILM PROPERTIES, F(T), VERSUS OXIDATION TEMPERATURE, $T_{ox}$

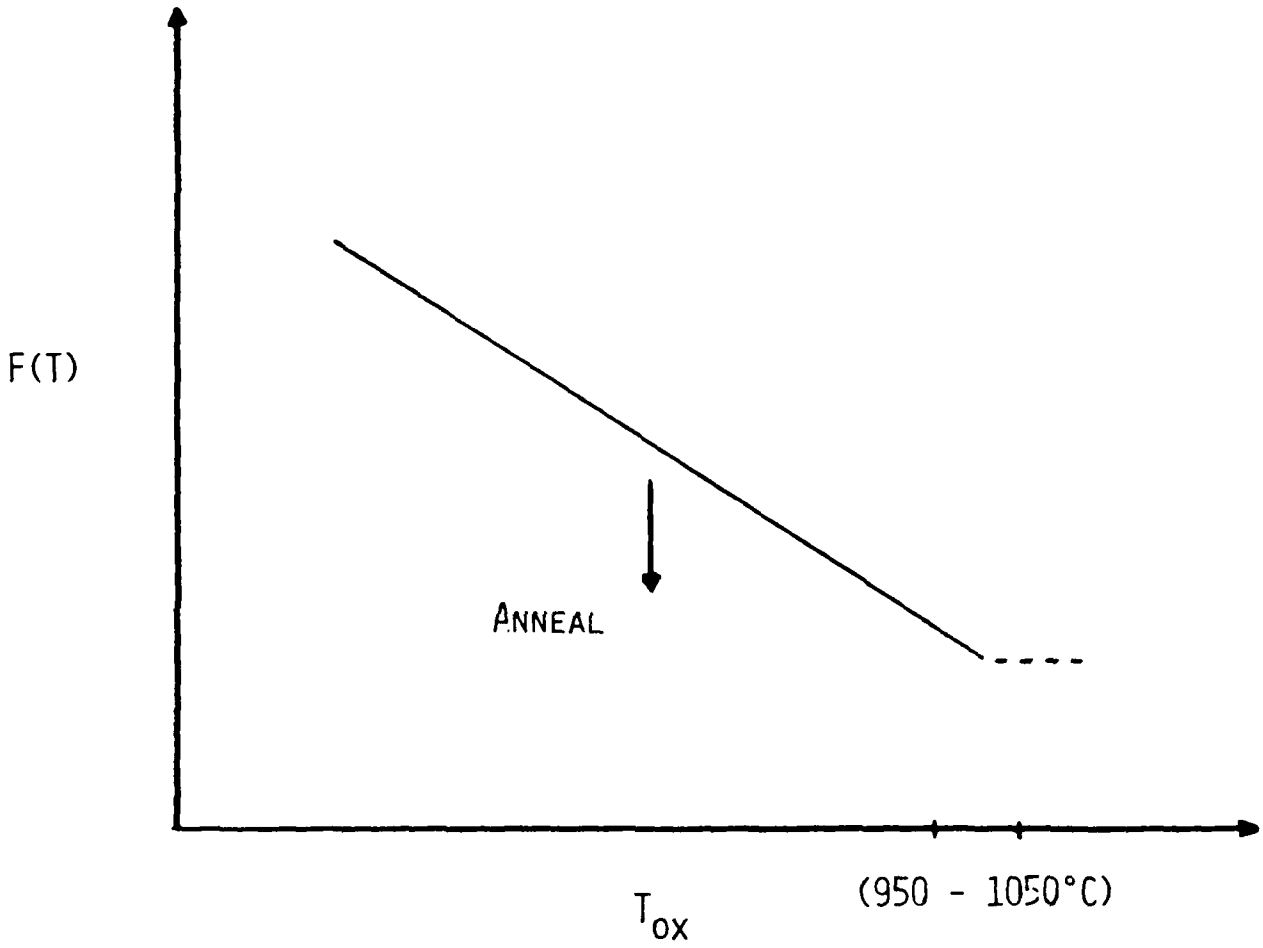


| F(T) | |
|---|---|
| INTRINSIC STRESS | $\sigma_i$ |
| DENSITY | $\rho$ |
| REFRACTIVE INDEX | N |
| FIXED OXIDE CHARGE | $Q_F$ |
| INTERFACE TRAPPED CHARGE | $Q_{IT}$ |

Fig 6

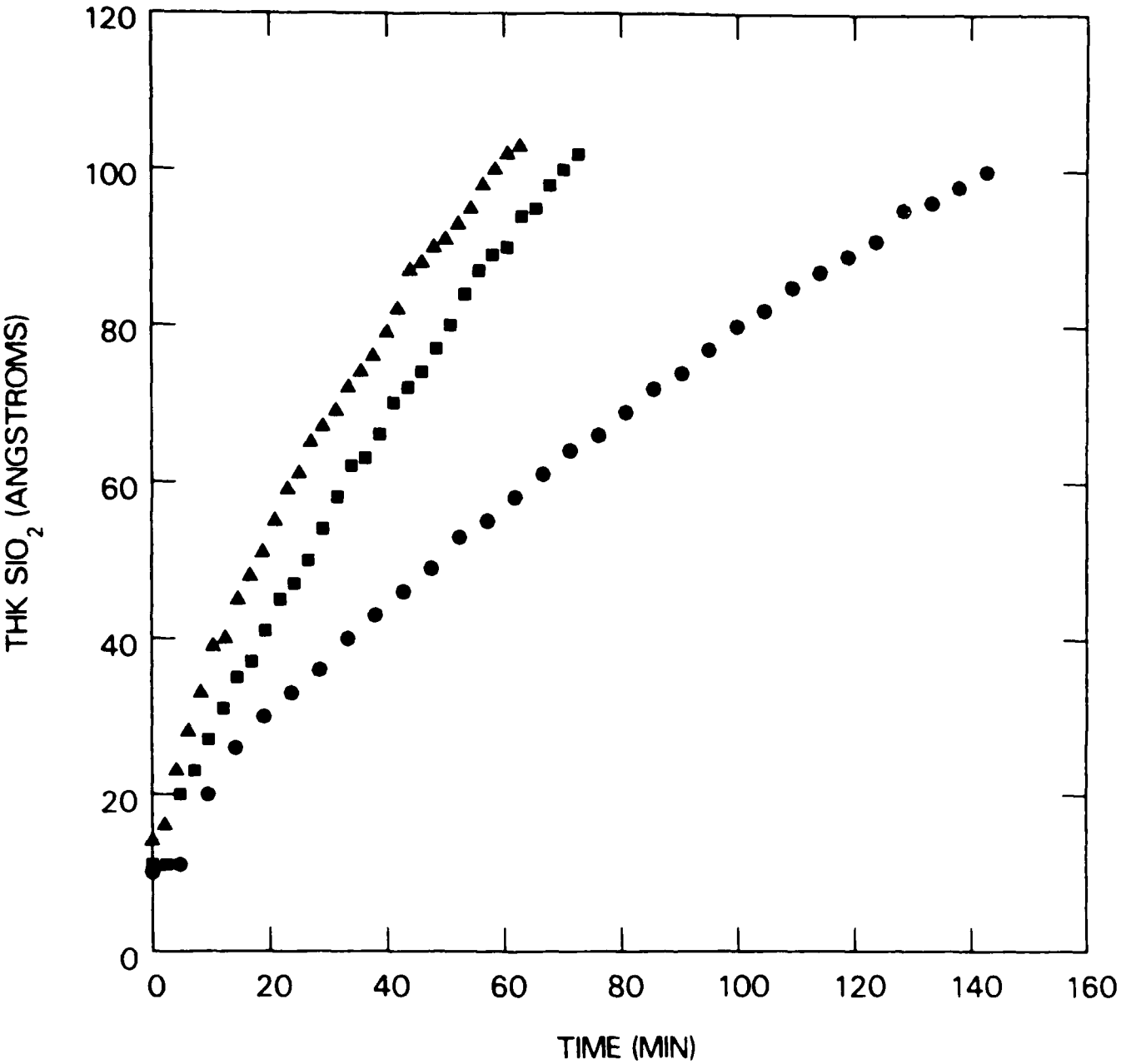
120
100
80
60
40
20
0
THK SIO2 (ANGSTROMS)
0
20
40
60
80
100
120
140
160
TIME (MIN)

Fig. 7a

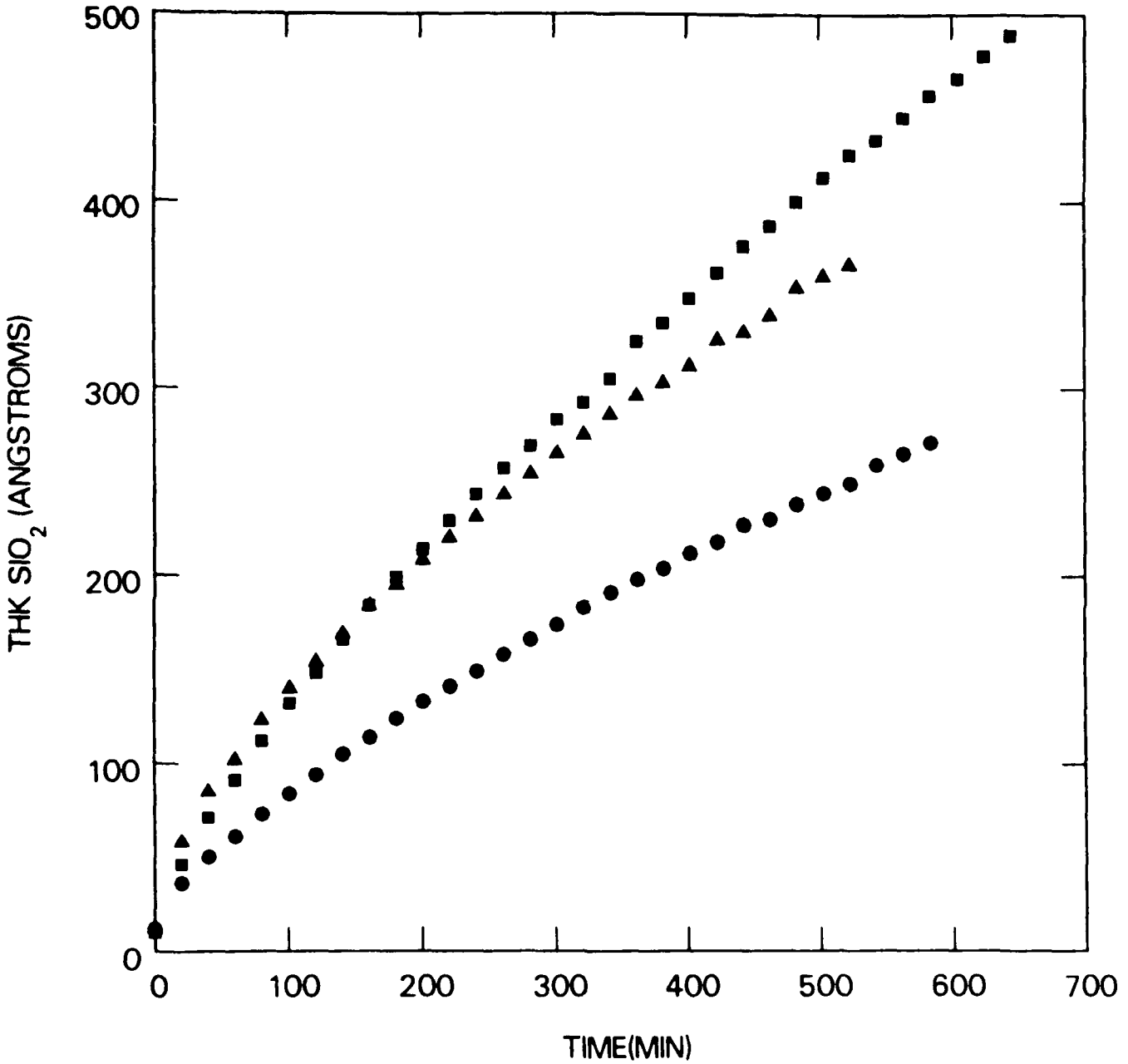
500
400
300
200
100
0
THK $SiO_2$ (ANGSTROMS)
0
100
200
300
400
500
600
700
TIME(MIN)

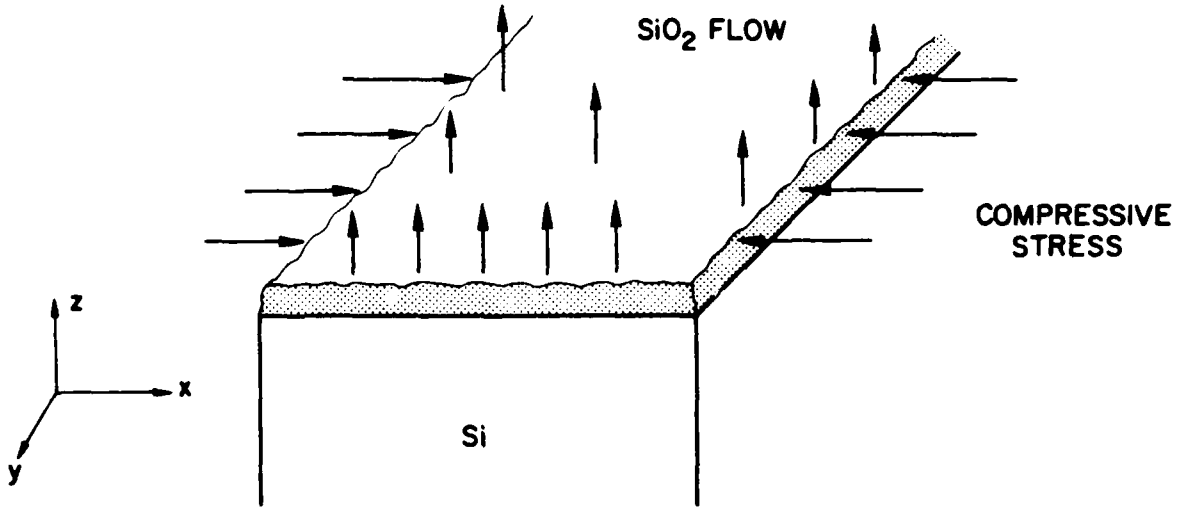


Fig 8

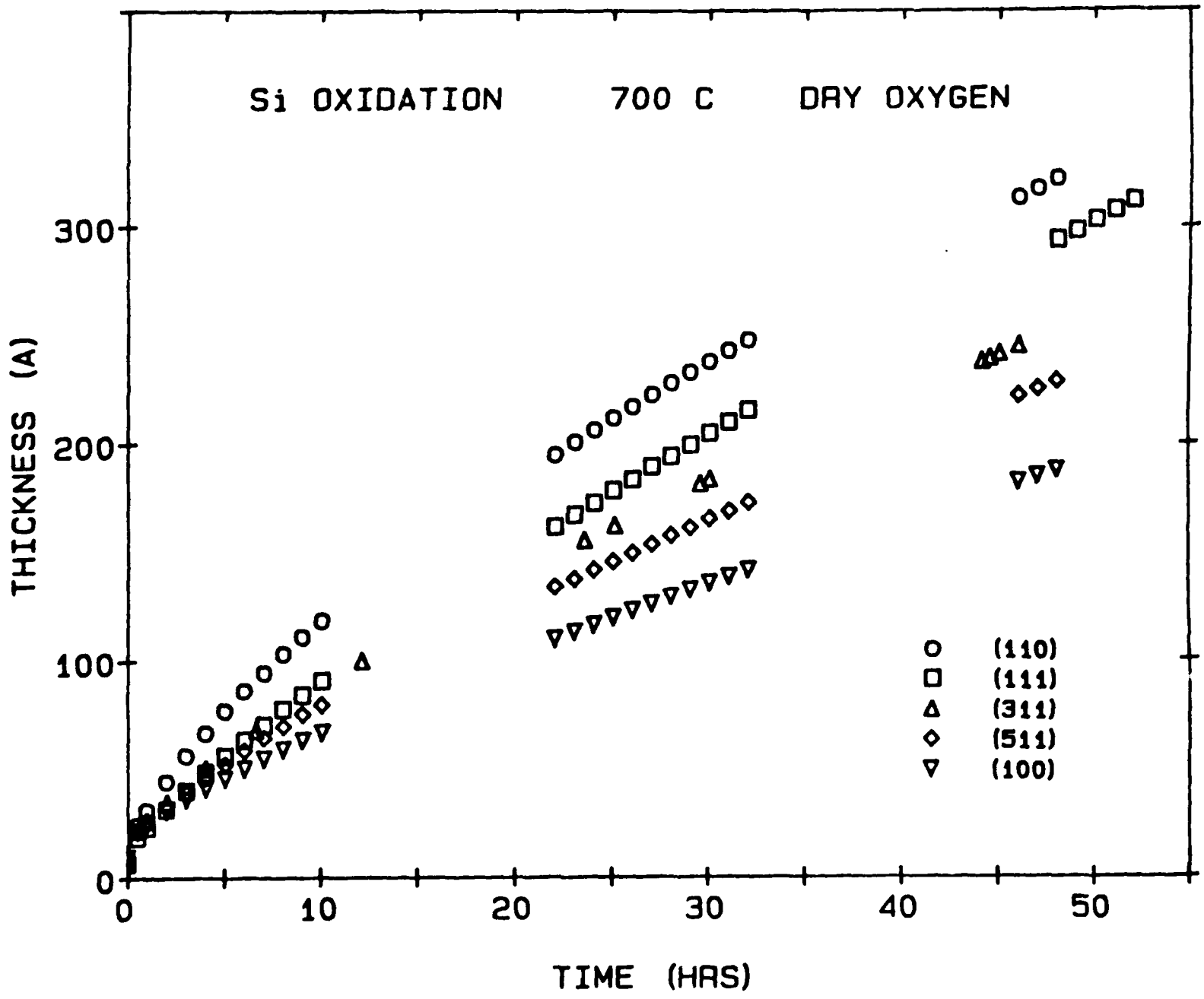
Si OXIDATION 700 C DRY OXYGEN
THICKNESS (A)
TIME (HRS)
0
100
200
300
0
10
20
30
40
50
(110)
(111)
(311)
(511)
(100)

Fig 9

STEP OXIDATION MODEL

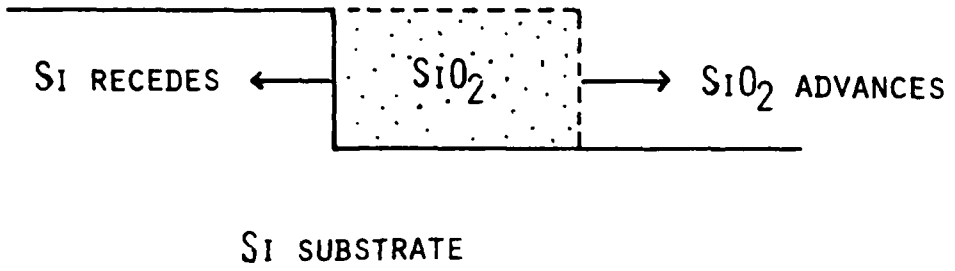


Fig. 10

END

DTIC

8-86